Leading Edge Flow by the Monte Carlo Direct Simulation Technique

F. W. VOGENITZ,* J. E. BROADWELL,† AND G. A. BIRD‡
TRW Systems Group, Redondo Beach, Calif.

The flow near the leading edge of a sharp flat plate is studied by means of a Monte Carlo molecular simulation. This technique consists of following, by digital computation, the motion of a representative set of molecules flowing past the body while collisions are computed by statistical sampling. Flowfield properties and plate surface fluxes are presented for a monatomic gas for several molecular models: hard spheres and point centers of inverse power repulsion. The gas-surface interaction law used was a prescribed mixture of diffuse and specular reflection. Mach number was varied from 5.5 to 29.2 and both insulated and cooled plates were studied. Plate length relative to the freestream mean free path was varied from 10 to 88. For the longer plates the flow over much of the plate is that for a semi-infinite plate. Comparisons are made between these results and experimental data.

Nomenclature

A	= hard sphere collision cross section
b	= impact parameter
F	= intermolecular force = $Kr^{-\nu}$
L^*	= L/λ_∞ plate length over mean free path
m^*	= reduced mass
M	= Mach number
n	= molecule number density
N_c	= number of molecules in cell
$\bar{p}$	= p/p_{fm} pressure ratio
$\bar{Q}$	= Q/Q_{fm} heat transfer ratio
Re_x	= $\rho_\infty U_\infty X/\mu_\infty$
S	= speed ratio $U/(2RT)^{1/2}$
t	= leading edge thickness
T^*	= T/T_∞ static temperature ratio
T_o	= freestream total temperature
U	= x component of velocity
V_r	= relative velocity
W_m	= dimensionless impact parameter cutoff
X,Y	= distance from leading edge, distance perpendicular to plate
X^*,Y^*	= X/λ_∞, Y/λ_∞
γ	= ratio of specific heats
ρ^*	= ρ/ρ_∞ density ratio

Subscripts

fm	= free molecule value for diffuse reflection
w	= wall value
∞	= freestream value

Presented as Paper 69-141 at the AIAA 7th Aerospace Sciences Meeting, New York, January 20–22, 1969; submitted January 30, 1969; revision received August 20, 1969. The authors wish to acknowledge the interest and support of the Advanced Research Projects Agency in this investigation. The work was administered through SAMSO Contract No. F04701-69-C0119. The authors thank G. Takata for his capable handling of the computer programing associated with this work. We also thank Becker, Horstman, Metcalf, Lillicrap, and Berry for making available copies of their papers presented at the Sixth Rarefied Gas Dynamics Symposium.

* Member of the Technical Staff, Fluid Physics Department. Member AIAA.

† Senior Staff Engineer, Aerosciences Lab. Associate Fellow AIAA.

‡ Consultant; also Professor of Aeronautical Engineering, University of Sydney. Member AIAA.

I. Introduction

THE nature of the flow near the leading edge of a sharp flat plate has long been a controversial matter. Recently, however, much detailed experimental information about the flow has been obtained, some of it describing the structure in regions as small as a few mean free paths in extent.

With regard to theory, it has been recognized that, for high Mach number at least, continuum equations are probably inadequate in this region, and there have been a few studies using kinetic theory. Charwat[1] considered first and second collisions in the region very near the leading edge of a sharp flat plate and estimated the trends in induced pressure and skin friction there by an approximate analytical procedure. Kogan[2] studied near-free molecule flow over a short plate by a Monte Carlo method, including only first collisions. The most extensive kinetic theory studies are those of Huang and co-workers[3,4] who claim to have found discrete ordinate solutions to the BGK approximation to the Boltzmann equation for a semi-infinite plate. However, we find the results of Ref. 3 to be substantially at variance with both our Monte Carlo results and experimental data. Although it is possible that the differences are due in part to the BGK model or the discrete ordinate procedure, it is our belief that the main source of the discrepancy is the use of an improper numerical method to solve a finite difference representation in two-dimensional physical space of the steady BGK model equation. The calculation procedure used in Ref. 3 is that of the initial value problem, i.e., starting upstream of the leading edge and marching downstream. Boundary conditions are applied upstream of the leading edge, at the plate and at infinite Y, where Y is distance normal to the plate. The calculation is iterated from the undisturbed uniform flow. No downstream boundary condition is applied and it is claimed that this is justified because "downstream flow properties do not significantly affect upstream flow properties in the hypersonic flow." Now it is true that for a highly cooled plate in hypersonic flow the influence of the portions of the plate downstream of any point extends upstream of that point for only a few mean free paths, as we will show in this paper. However, the cumulative effect of upstream molecular motion along the entire length of the plate is not small, and cannot be neglected. The result of neglecting it can be seen in the solutions of Huang and Hwang; the disturbance fails to grow properly in strength with distance from the leading edge. In addition, the finite difference step sizes in the stream direction used in Ref. 3 were $\Delta X^* = 5$ for $0 \leq X^* \leq 10$ and $\Delta X^* = 10$ for $10 < X^* < 50$. These are quite large compared to the gradients in the leading edge region and this may have contributed to the error in disturbance strength. Some of the results from Ref. 3 that led to these conclusions are discussed in following sections.

Huang[5] found solutions for a finite plate by a procedure similar to that described above, with the important difference that freestream conditions are prescribed at infinity downstream of the plate trailing edge. The distribution function for upstream molecular velocities is then found by marching upstream from this rear boundary with a finite difference technique and iterating. However, macroscopic properties were presented in Ref. 5 only for plates $2\lambda_\infty$ in length and no appropriate comparison can be made with our results.

In the present work, the flow past plates up to 88 mean free paths long is examined by means of a numerical method which makes no assumptions about the form of the distribution function. Thus, it can deal with the highly nonequilibrium aspects of the flow that arise near the leading edge and that are especially important at high Mach number. In the Monte Carlo simulation technique the Boltzmann equation is not written down and explicitly solved. However, the arguments used to construct the simulation procedure are very similar to those used to derive the Boltzmann equation. Hence the Monte Carlo solutions are believed to constitute numerical solutions to the Boltzman equations.

II. Monte Carlo Direct Simulation Technique

The numerical method applied in the present work has been described in various stages of recent development in Refs. 6–8. Briefly, the technique consists of describing, by digital computation, the motion of a set of molecules as they move past the body. Molecules are steadily inserted into the flowfield upstream of the body and leave at a downstream boundary, several thousand being in the field at any one time. The molecular motions are followed exactly but the collisions are treated by statistical sampling. Reference 7 contains a detailed description of the procedure.

In Ref. 7 only hard sphere molecules were treated; here point centers of inverse power repulsion are considered as well. For the latter, two force laws were used: $F = Kr^{-5}$ and Kr^{-12}. The modifications to the M-C procedure for these models are as follows.

1) Pairs of molecules are selected at random and are retained for collision with probability proportional to their relative velocity raised to an exponent m whose value depends upon the molecular model. For hard spheres $m = 1$. For molecules repelling with the force law $F = Kr^{-\nu}$, $m = (\nu - 5)/(\nu - 1)$.

2) For pairs of molecules which have been accepted for collision, a line of impact and azimuth angle in the center of mass reference frame are selected and the conservation laws are applied. For hard spheres the scattering is isotropic in this reference frame. For power law molecules the dimensionless impact parameter $W = b(K/m^*v_r^2)^{-1/\nu-1}$ is selected with probability $\sim W$. The new direction of the relative velocity vector is found from the deflection integral.[9] The range of impact parameter W is truncated at a maximum value which corresponds to a deflection angle of approximately 10°. Collisions producing deflections smaller than this are neglected as contributing negligibly to transport. (Most of the calculations for 12th power molecules presented here were made with an earlier scheme in which the cutoff is done in impact parameter, b, in physical space, not in deflection angle. This is slightly less rigorous in that encounters with large b, which can result in a large deflection if V_r is very small, are neglected. These occur relatively infrequently, and a comparison of results of the two schemes reveals no significant differences.)

3) At each collision, a time counter for the cell in which it occurs is advanced by an appropriate amount. For hard spheres $\Delta T_N = 2/N_c(AnV_r)^{-1}$. For power law molecules

$$\Delta T_N = 2/N_c[\pi W_m{}^2(K/m^*)^{2/(\nu-1)}nV_r{}^{(\nu-5)/(\nu-1)}]^{-1}$$

where ΔT_N = time increment for the collision.

This sampling scheme produces a collision frequency for pairs of molecules proportional to the product of the local number density and the relative velocity of the pair, raised to the appropriate exponent. The resulting distance that molecules move between collisions is a distributed quantity whose average is equal to the local mean free path. The collision frequency and mean free path produced by this collision process have been studied previously.[10]

In addition to the net force and heat transfer to the body, the method provides a detailed description of the flow; viz, 1) flowfield properties: density, temperature, velocity, etc., everywhere in the region surrounding the body; 2) local values on the body surface of pressure, skin friction, number flux, heat transfer, etc.; 3) the distribution function everywhere in the gas.

III. Boundary Conditions

The boundary condition applied at the rear edge of the field is that which would be exact if there were no streamwise gradient in the distribution function for negative (upstream) molecular velocities, as in free molecule flow. Imagine physical space downstream of the rear boundary of the field to be populated with a collection of molecules which is the mirror image (in physical space) of the collection upstream of the boundary. (Only the upstream moving molecules need be represented.) If during the movement interval, ΔT_M, a molecule in the field moves upstream an X distance greater than its initial distance from the boundary, its mirror image would then move inside the field.

For the plate lengths studied here, there obviously is a streamwise gradient in the entire velocity distribution in the wake of the plate; however, the error introduced by employing this boundary condition is made negligible by placing the rear field boundary $\sim 10\lambda_\infty$ downstream from the plate trailing edge where the flow is strongly supersonic.

The same kind of boundary condition could be used at the upper edge of the field, i.e., uniformity in the Y direction for the distribution function for molecular velocities directed toward the plate. No error is then incurred if the upper edge is set far enough from the plate to completely contain the disturbance. For these calculations a modified version of this condition is used in which entering molecules with velocities not likely to have come from the uniform freestream distribution are removed from the calculation. This introduces a slight spurious reflected disturbance which invalidates the results very near the boundary, but it allows the boundary to be set closer to the plate, reducing storage requirements. Calculations have been made both with the boundary set so as to include all of the disturbance and with it located closer to the plate. In the latter case, the part of the flowfield affected by the boundary is discarded. The flux of molecules across the upstream boundary is maintained at that appropriate to the freestream.

IV. Statistical Fluctuations

The value of any quantity computed with this technique has a sample size (the number of molecules involved) and standard deviation associated with it. The standard deviation σ should decrease roughly inversely as the square root of sample size, but it is impossible to make accurate a priori estimates of expected scatter. Therefore, calculations were made with the simulated gas flowing without a disturbance (reflection from the plate surface made completely specular).

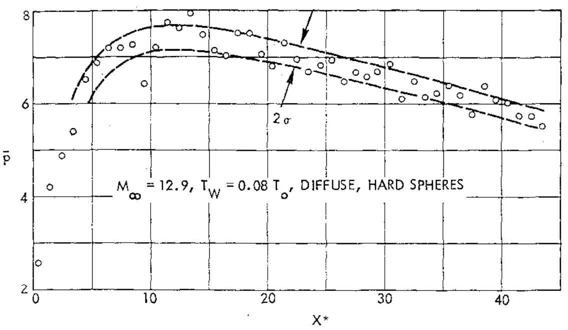

Fig. 1 Statistical fluctuation and standard deviation-plate pressure.

The scatter was found to be close to Gaussian with standard deviation as shown in the table below. Sample sizes for most of the calculations presented here are within the range shown in the table.

The plate surface is divided into segments approximately equal in length to λ_∞ and a cumulative average of the flux of energy and momentum to each segment is recorded. What results then for a quantity such as plate pressure is a sequence of points as shown in Fig. 1, each of which represents the average pressure on a segment. It can be seen that most of the points fall within a band formed by applying the (independently estimated) standard deviation to a faired mean. The sample size for this calculation was 1000, i.e., approximately 1000 molecules struck each segment. All results of our calculations shown elsewhere in this paper are mean curves faired through the scatter by eye.

V. Results

All the computations were made for plates of finite length L, and describe the flow downstream as well as upstream of the plate. In addition to a disturbance extending forward of the leading edge, there is an effect of the trailing edge on the aft section of the plates. The wake and trailing edge effects are not the primary subject of the present study, but the latter will be discussed briefly after the main results have been presented. These, except where otherwise noted, are all outside the influence of the trailing edge and are, therefore, those that would be obtained on a semi-infinite plate.

Of the three molecular models employed in the calculations, the 12th power law is believed to be the most realistic but the results produced with it differed but little from those for the hard spheres. Therefore, because it requires somewhat shorter computation times, the hard sphere model was used in most calculations. The results except where otherwise noted are for this case. The influence of the molecular interaction law on plate pressure is discussed in a separate section.

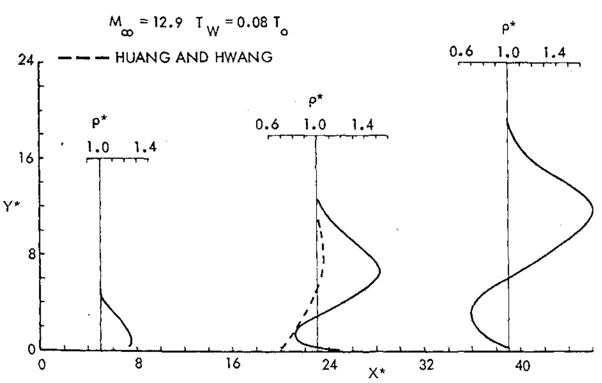

Fig. 2 Shock wave development on plate.

The gas-surface interaction law employed was a prescribed mixture of diffuse and specular reflection. Unless otherwise noted all results presented are for the completely diffuse case.

Results at $M_\infty = 12.9$

The Monte Carlo model as presently formulated is restricted to single point centers of repulsion and is, therefore, most directly applicable to monatomic gases. For this reason, the most extensive calculations were made for $M_\infty = 12.9$ and $T_w = 0.08T_o$ to match the conditions chosen by Becker[11] in his study of argon (and nitrogen) flow past a sharp plate. There were for Ar: $M_\infty = 12.66$, $T_w = 0.08T_o$; and for N_2, $M_\infty = 11.18$, $T_w = 0.1T_o$.

Figure 2 shows the computed density profiles on a plate of length, $L^* = L/\lambda_\infty = 48$, for a hard sphere molecular model. The generation of a shock wave of growing strength is clearly shown. This characteristic is now well known from the measurements of McCroskey, Bogdonoff, and McDougall[12] and of others.

As is illustrated by the curves at $X^* = X/\lambda_\infty = 23$, the maximum density as well as the profile shapes predicted by Huang and Hwang[3] differ significantly from the M-C values.

Figure 3 compares the computed plate pressure with Becker's argon and nitrogen data, and the important effect of allowing 30% of the molecules to reflect specularly is also shown. We see that the theoretical pressure exceeds the free molecule value at the leading edge, rises to a peak and then begins to decrease as it does in interaction theory. Near the leading edge, the pressure decreases in direct proportion to the percent specular reflection, indicating that the normal force on the wall arises primarily from the deflection of molecules with nearly freestream velocity onto the plate.

In view of the importance of the unknown gas-surface interaction and possible plate bluntness effects discussed later, a comparison between the theory and measurements near the leading edge may not be meaningful. However, these effects decrease with distance from the leading edge and the agreement at greater X^* between the argon data and the calculations is significant.

With regard to the agreement of the computed values with the N_2 results there is, of course, the additional question concerning the internal degrees of freedom. Perhaps their effect on pressure is small but it is also possible that the rotational modes are not excited in the first few mean free paths from the leading edge. In the present circumstances, ~ 10 collisions are required to equilibrate the rotational modes in N_2.[13] Thus N_2 could act as a monatomic gas in the first few mean free paths, especially when the cold wall de-excites the molecules which strike it.

The sharp decrease in pressure in Fig. 3 for $X^* < 10$ is not predicted in Ref. 3. Instead, the pressure is nearly constant in the region $1 \lesssim X^* \lesssim 10$. In addition, that analysis shows

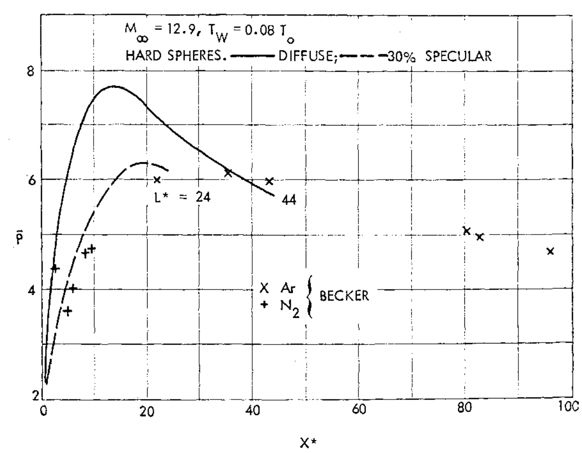

Fig. 3 Plate pressure relative to free molecule value.

Table 1 Standard deviation

Property	Sample size	Standard deviation
Plate pressure, etc.	350	$\sigma_x = 7\% \ x$
	1000	3%
Flowfield density,	1300	4%
temperature, etc.	4500	3%

the pressure to decrease when T_w is raised. The opposite effect is given by the M-C method. This can be deduced from a comparison of Figs. 3 and 12, where $p_{fm}/p_\infty = 1.55$ and 4.23, respectively.

Figure 4 shows the generally similar behavior of heat transfer. This figure also serves to represent shear stress, relative to the free molecule value; for throughout the region shown, there is no discernible difference in the magnitudes of the two properties (referenced to their free molecule values).

In Fig. 5 are shown the outer edges of the disturbance and the maximum density locations, the latter for both hot and cold walls. Also indicated are the disturbance boundaries determined from Becker's wire surveys as well as that for $M_\infty = 26$ measured by Joss, Vas, and Bogdonoff.[14] It is difficult to define these boundaries with any precision. In the experiments the instrument sensitivity is crucial, and in the calculations the fluctuations obscure the weak gradients at the edges. Furthermore, the change in one flow property may be more apparent than in another. The lines marked temperature and density thickness illustrate this point; they mark the places at which the two properties first rise noticeably out of the freestream fluctuations. These considerations make it difficult to compare the theory and experiment, but it is clear that the disturbance measured by Joss et al., is much thicker than the Monte Carlo prediction. While less clear, it also appears that Becker's disturbance in argon is growing with X faster than in the theory. It is possible that both these differences are attributable to a combination of leading edge "bluntness" and finite wedge angle in the experiments.

Although the leading edge thickness in Becker's case was extremely small by any proposed standards for rarefied gas experiments, about $\frac{1}{20}\lambda_\infty$ in argon and $\frac{1}{180}\lambda_\infty$ in nitrogen, the following considerations suggest that it may have had an effect in the argon flow. The nature of the disturbance at a distance of say $10\lambda_\infty$ from the leading edge is determined by the reflection of molecules from the plate upstream of that point. The M-C calculations show that the impingement rate on the wall in this region is only about twice the free molecule value. Thus, the ratio of the flux to a normal leading edge, t thick, to that on a length l of the plate is $\sim 2M_\infty \cdot t/l$. Therefore, in the argon experiment (but not in nitrogen), the flux to the leading edge was of the same order as that to the first few mean free paths of plate length. The largely forward emission from the edge compared to the lateral flow from the sides enhances the effect of the edge as would any trend of the accommodation coefficient toward the specular.

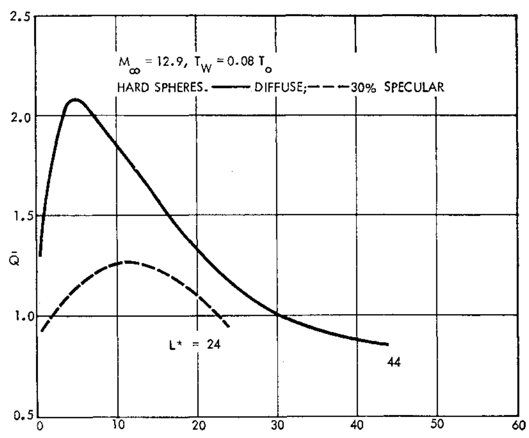

Fig. 4 Plate heat transfer rate relative to free molecule value.

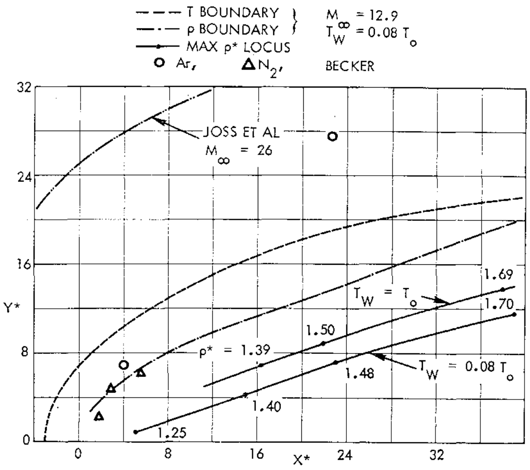

Fig. 5 Disturbance boundaries and maximum density loci.

The standard for sharpness implied by these remarks is much higher than that stated by Joss et al., who found that even at $M_\infty = 26$ $t < \frac{1}{4}\lambda_\infty$ was sufficient. However, the angle of their plate lower surface was 20° compared to Becker's 15°, and the argument just given implies that the requirement is angle dependent: at a given angle, an edge thickness is reached below which reflection from the lower surface overshadows that from the leading edge. Preliminary computations for a sharp plate with a 20° lower surface indicate that the disturbance is indeed much thicker than that for a zero thickness plate. However, more experiments as well as more extensive calculations will be required before the matter can be resolved.

Another point of interest in Fig. 5 is the fact that a large wall temperature increase shifts the line of maximum density outward only slightly and leaves the maximum density at a given X^* relatively unchanged. This behavior has been noted by Metcalf, et al.,[15] and is discussed further in connection with their measurements.

The data in Fig. 6 are intended first to emphasize the distance from equilibrium and hence from a Navier-Stokes regime in the flow at the farthest aft station (free from the trailing edge influence) in the present case. T_x is kinetic temperature computed from the x component of the random molecular motion (relative to the fluid velocity) and differs little from T itself through the weak shock wave. Near the plate, however, the difference is enormous.

The temperature gradient in the gas at the wall reverses between the stations $X^* = 9$ and $X^* = 39$ while as the next

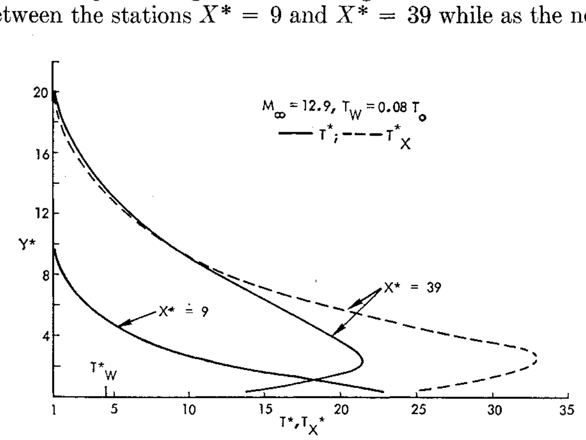

Fig. 6 Temperature profiles.

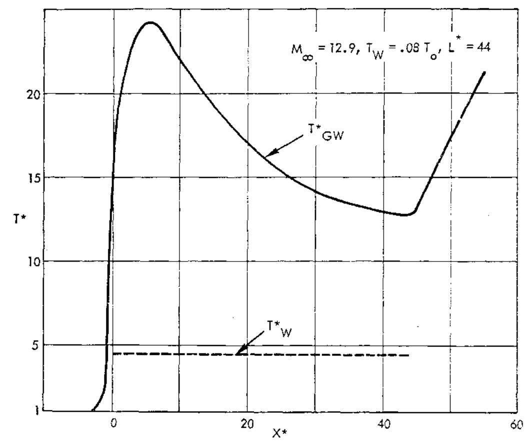

Fig. 7 Gas temperature near wall.

figure, Fig. 7, shows the gas temperature near the wall, T_{GW}, exceeds the wall temperature throughout the region. Thus the temperature jump at the wall cannot be proportional to the gradient.

Results at $M_\infty \simeq 6$ and 30

Metcalf et al., have made electron beam density measurements in nitrogen on a plate at two wall temperatures at $M_\infty \simeq 6$. Figures 8–10 show the comparison with the Monte Carlo results.§ At the two downstream locations, $X^* = 9$ and 18, Figs. 9 and 10, most of the experimental features are reproduced by the M-C computation. In addition to the agreement between the disturbance strength and location, there is also a similar response of the profiles to the change in wall temperature. The discrepancy in the density near the wall almost certainly arises from the difference in T_w/T_∞ between theory and experiment that occurs, because of the γ difference, when T_w/T_o is matched. That these T_w differences have little effect on the outer parts of the profiles is seen to be consistent with both the experimental and computed effect of a T_w change.

At $X^* = 5$ the measured disturbance is much stronger and thicker than the computed one. It is natural to attribute this difference to the finite leading edge thickness and wedge angle of the model but since the former is not reported this is a conjecture.

§ In these figures X^* was computed from the relation $X/\lambda_\infty = (2/\gamma\pi)^{1/2}\cdot Re_x/M_\infty$ which follows from the hard sphere relation for viscosity.

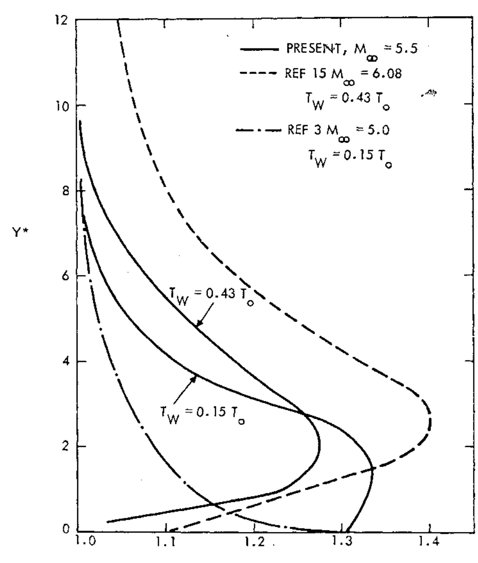

Fig. 8 Density profiles at $X^* = 5$.

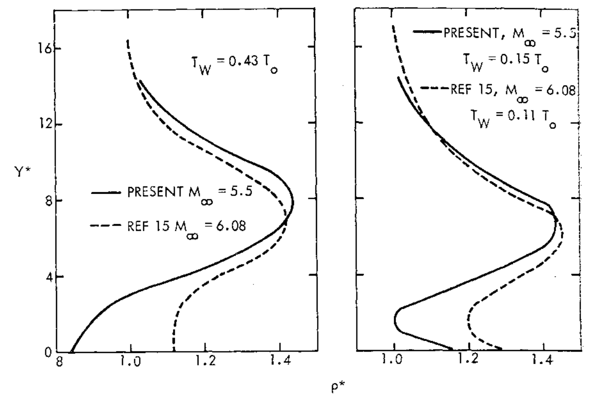

Fig. 9 Density profiles at $X^* = 9$.

It should be pointed out again that the very satisfactory agreement between the theory and these experiments, although encouraging, is not conclusive because of the unknown role of γ in this regime.

In Fig. 8 the profile taken from Ref. 3, for $M_\infty = 5$ and $T_w/T_o = 0.15$, is also shown. The next downstream stations for which these authors give results is $X^* = 50$ where they predict the maximum density ratio ρ^*, to be 1.1. The M-C calculation does not extend this far aft but the value measured by Metcalf et al., at $X^* = 54.5$ for $T_w/T_o = 0.11$ is $\rho^* = 1.61$.

Figure 11 compares computed plate pressure with data for another monatomic gas, helium, at $M_\infty \simeq 30$ and $T_w = 0.72T_o$, presented in Ref. 16. Here again the pressure levels are in approximate agreement, but the measurements do not extend close enough to the leading edge to locate the peak. The experimental results fall in two bands and hence, as Horstman points out, there is an effect of Reynolds number per inch in the data. For his model at the aforementioned conditions, $t/\lambda_\infty \sim \frac{1}{30}$ so the effect again may be from leading edge thickness. Note that the effect of 30% specular reflection becomes negligible for $X^* > 70$.

Effect of Molecular Model

Three molecular models have been investigated: hard spheres and point centers of inverse power repulsion with (force) exponent 12 and 5. For the power law models the collision cross section varies inversely as a power of the relative velocity of encounter, the variation becoming larger as the exponent ν in the force law becomes smaller. The constant K in the force law is determined in terms of the hard sphere collision cross section by matching the freestream viscosity of the hard sphere gas. This produces an effective mean free path (based on viscosity cross section) in the freestream which is very nearly identical for all the models at the same freestream density and temperature.

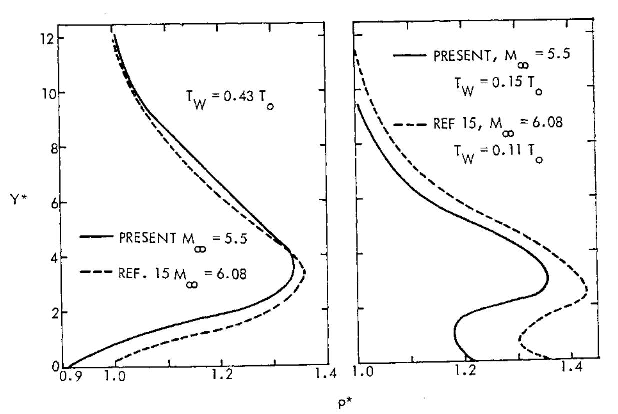

Fig. 10 Density profiles at $X^* = 18$.

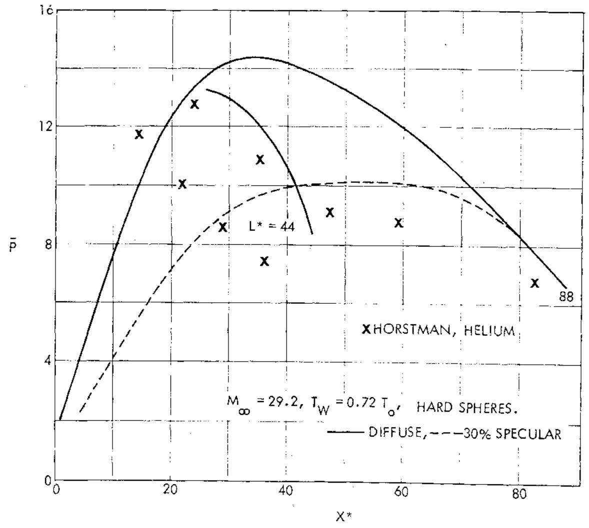

Fig. 11 Plate pressure relative to free molecule value.

In Fig. 12 plate pressure for the three models at M_∞ = 12.9, $T_w = T_o$ is plotted against distance normalized by freestream mean free path. The softest model is seen to have the least rapid rise in induced pressure. The gross differences are, of course, attributable to differences in the molecular free paths in the disturbance and it is clear that these results can be correlated to some extent by scaling distance with some effective mean free path in the disturbance. However, this can only be approximate; the flows for the various models are different in detail. In addition, the density and temperature upon which to base a mean free path to produce some kind of "best agreement" could only be found by trial and error.

Real gases, of course, differ in their rate of collision cross section variation and it seems appropriate for our purposes to compare the molecular models using λ_∞ and to view the differences as those we might expect to find among various real gases.

Recent experiments[17] in argon in the temperature range 1500–4800°K suggest a value for the viscosity-temperature exponent of 0.68, which corresponds to a force law exponent of 12. Moreover, a plane shock wave density profile computed with this Monte Carlo technique for 12th power molecules is in excellent agreement with an experimental profile for a Mach 8 shock in argon,[8] hence there is some reason to believe the 12th power molecules adequately represent the properties of argon at moderate to high temperatures. However, we find that twelfth power molecules produce a result only slightly different from that for hard spheres and thus the latter results can usefully be compared with experimental data in most monatomic gases at moderate to high temperatures.

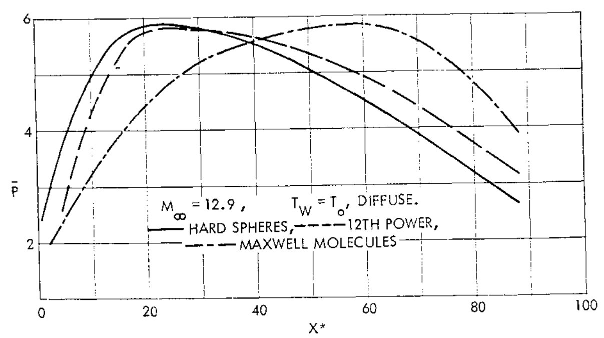

Fig. 12 Molecular model effect on plate pressure.

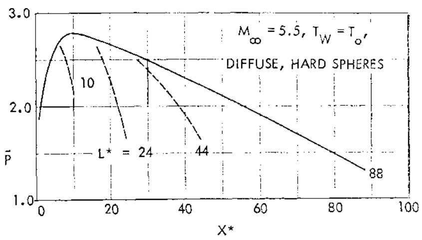

Fig. 13 Plate length effect on pressure.

Effect of Finite Plate Length

Calculations were made for plates of length, L^*, from 10.0 to 88.0. The effect of the trailing edge is found to vary considerably depending upon the property under consideration and the freestream Mach number and plate temperature.

At M_∞ = 5.5, the pressure on an insulated plate is reduced noticeably near the trailing edge, the extent of the affected region increasing as the plate length increases as shown in Fig. 13. However, for this condition there is no discernible trailing edge effect on shear stress. The variation with X of velocity near the plate is plotted in Fig. 14. An expansion extending over a few mean free paths at the trailing edge and the rapid increase of velocity in the wake can be seen. For the cooled plate ($T_w = 0.08T_o$) at Mach 12.9 the trailing edge effect is so small as to be just barely discernible in some flow properties. Trailing edge effects for the other flow conditions reported on here fall somewhere between these two extremes, i.e., low Mach number and high plate temperature increase trailing edge effects—high Mach number and low plate temperature decrease them.

In general it can be said that the effect of the trailing edge on the flow upstream of the trailing edge is confined to a region near the plate surface and extending, at the most, a distance of the order of 10 mean free paths upstream. Therefore, for the greater plate lengths studied here the flow over much of the plate is that for a semi-infinite plate.

VI. Summary and Conclusions

What has been presented here is a very detailed description of the formation of the flow in the vicinity of a sharp leading edge determined by a theoretical method which properly accounts for nonequilibrium effects, i.e., which makes no assumptions about the form of the distribution function. At $M_\infty \sim 13$ and $T_w \sim 0.10T_o$, such effects are still large at least $40\lambda_\infty$ from the leading edge.

Comparison has been made with experimental data and the over-all picture of the flow produced by the theory is in good agreement with that arising from the measurements. A few flow features are not in agreement with the data, and it may be that the data are influenced by factors not represented in the theory. In particular, leading edge thicknesses

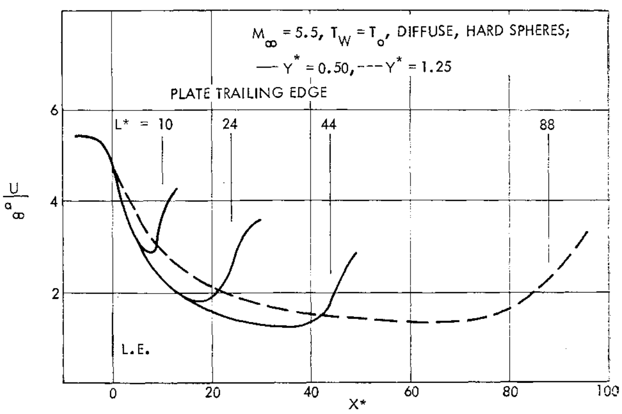

Fig. 14 Gas velocity near surface.

small compared to λ_∞ and small lower surface angles may still have important effects on high Mach number leading edge flows. In addition, at $M_\infty \sim 13$, the nature of the gas-surface interaction is found to have large influences on the flow in the regions extending as far downstream as $25\lambda_\infty$ from the leading edge. Therefore, for properties such as plate pressure very near the leading edge, it would be inappropriate to claim agreement or disagreement. In the case of flowfield properties only weakly influenced by these factors, the qualitative agreement in trends and quantitative agreement in magnitudes is found to be good.

The Monte Carlo technique is presently being extended to include diatomic gases, and comparison with the numerous existing measurements in such gases will be worthwhile. However, more experimental data for monatomic gases near the leading edge would be welcome.

No attempt has been made to classify the flow as to different regimes and the data are presented in terms of the parameters appropriate in kinetic theory, not the customary continuum interaction parameters. It is clearly important to connect these results with earlier studies, both theoretical and experimental, and to determine the proper set of parameters and point of view for the flow regions extending from the leading edge to the beginning of the interaction regime.

References

[1] Charwat, A. F., "Molecular Flow Study of the Hypersonic Sharp Leading Edge Interaction," *Rarefied Gas Dynamics*, edited by L. Talbot, Academic Press, New York, 1961, pp 553–578.

[2] Kogan, M. N. and Degtyarev, L. M., "On the Computation of Flows at Large Knudsen Numbers," *Astronautica Acta*, Vol. 11, No. 1, 1965, pp. 36–42.

[3] Huang, A. B. and Hwang, P. F., "Kinetic Theory of the Sharp Leading Edge Problem II. Hypersonic Flow," paper RE63, Oct. 1968, International Astronautical Federation, New York.

[4] Huang, A. B. and Hartley, D. L., "Kinetic Theory of the Sharp Leading Edge Problem in Supersonic Flow," *The Physics of Fluids*, Vol. 12, No. 1, Jan. 1969, pp. 96–108.

[5] Huang, A. B., "Kinetic Theory of the Rarefied Supersonic Flow over a Finite Plate," *Rarefied Gas Dynamics*, Suppl. 5, Vol. I, 1969, edited by L. Trilling and H. Wachman, Academic Press, New York, pp. 529–544.

[6] Bird, G. A., "The Velocity Distribution Function within a Shock Wave," *Journal of Fluid Mechanics*, Vol. 30, Pt. 3, Nov. 1967, pp. 479–489.

[7] Vogenitz, F. W. et al., "Theoretical and Experimental Study of Low Density Supersonic Flows about Several Simple Shapes," *AIAA Journal*, Vol. 6, No. 12, Dec. 1968, pp. 2388–2394.

[8] Bird, G. A., "Direct Simulation Monte Carlo Method-Current Status and Prospects," *Rarefied Gas Dynamics*, Suppl. 5, Vol. I, 1969, edited by L. Trilling and H. Wachman, Academic Press, New York, pp. 85–98.

[9] Present, R. D., *Kinetic Theory of Gases*, McGraw-Hill, New York, 1958, Chap. 8.

[10] Bird, G. A., "Approach to Translational Equilibrium in a Rigid Sphere Gas," *The Physics of Fluids*, Vol. 6, No. 10, Oct. 1963, pp. 1518–1519.

[11] Becker, M., "Flat Plate Flow Field and Surface Measurements in Low Density Argon Flow between Continuum and Near Free Molecule Flow," *Rarefied Gas Dynamics*, Suppl. 5, Vol. I, edited by L. Trilling and H. Wachman, Academic Press, New York, 1969, pp. 515–528.

[12] McCroskey, W. J., Bogdonoff, S. M., and McDougall, J. G., "An Experimental Model for the Sharp Flat Plate in Rarefied Hypersonic Flow," *AIAA Journal*, Vol. 4, No. 9, Sept. 1966, pp. 1580–1588.

[13] Parker, J. G., "Rotational and Vibrational Relaxation in Diatomic Gases," *The Physics of Fluids*, Vol. 2, No. 4, July-Aug. 1959, pp. 449–462.

[14] Joss, W. W., Vas, I. E., and Bogdonoff, S. M., "Studies of the Leading Edge Effect on the Rarefied Hypersonic Flow over a Flat Plate," AIAA Paper 68-5, New York, Jan. 1968.

[15] Metcalf, S. C., Lillicrap, D. C., and Berry C. J., "A Study of the Effect of Surface Condition on the Shock Layer Development over Sharp Edged Shapes in Low Reynolds Number High Speed Flow," *Rarefied Gas Dynamics*, Suppl. 5, Vol. I, edited by L. Trilling and H. Wachman, Academic Press, New York, 1969, pp. 619–634.

[16] Horstman, C. C., "Surface Pressures and Shock-Wave Shapes on Sharp Plates and Wedges in Low-Density Hypersonic Flow," *Rarefied Gas Dynamics*, Suppl. 5, Vol. I, edited by L. Trilling and H. Wachman, Academic Press, New York, 1969, pp. 593–605.

[17] Matula, R. A., "High Temperature Thermal Conductivity of Rare Gases and Gas Mixtures," *Journal of Heat Transfer*, Aug. 1969, pp. 319–327.